Evaluation of a 250kW-20,000min^{-1} High-Speed PM Motor

Takashi Okitsu,
Sho Uchiyama,
Keisuke Matsuo,
Daiki Matsuhashi

Keywords PM motor, High-speed rotation, Loss separation

Abstract

For high-speed fluid machinery like fans, blowers, and compressors, high-speed rotation is required to achieve a high energy conversion efficiency.

Aiming at applying to such high-speed application, we have developed a prototype of 250kW-20,000min^{-1} Permanent Magnet synchronous motor (PM motor) using an active magnetic bearing system. By applying the high speed PM motor to such applications, it will be realized of replacing the conventional system using speed increasing gear with direct drive system with eliminating the gear, so that making the system size compact, improving the system efficiency, and reducing the time of maintenance can be merit.

As a result of performance evaluation of the prototype, we confirmed that the motor efficiency at the rated point was 96.6% and the maximum efficiency in the whole motor operation range was 97.5%, and that the temperature rise of each part was lower than the specific value by performing heat run test.

Further, we have performed loss separation on prototype for improving the design accuracy toward a development of higher efficiency, speed, and larger capacity PM motor.

1 Preface

According to the government policy for the Climate Change, the demand for energy conservation has increased and the applications which incorporates Permanent Magnet synchronous motors (PM motors) with features of compact size and high efficiencies have been prominent in various industrial fields[(1)].

Aiming at applying to high-speed fluid machinery such as turbo-blowers, compressors, and refrigerators, we have developed a prototype of 250kW-20,000min^{-1} high-speed PM motor using an Active Magnetic Bearing (AMB)[(2)]. When this motor is applied to high-speed fluid machinery, a direct driving can be realized for a system where speed-increasing gears were formerly used and the following advantages can be obtained:

(1) Simple and compact system configuration. (Space saving)
(2) High system efficiency due to no gear loss (Energy conservation)
(3) Oil-free (Easy maintenance)
(4) Reduction of vibration and noise due to non-contact rotation.

On the other hand, although making the motor size compact and increasing output power density will be realized by high-speed rotation, it will lead to high loss density of the motor. Consequently, they will be an issue to reduce the motor loss and to choose a proper cooling system. In this paper, we present the characteristics of the prototype high-speed PM motor and the result of the loss and the temperature rise evaluation[(3)(4)].

2 Motor Specifications

Table 1 shows specifications and Fig. 1 shows a cross sectional configuration of the prototype of the high-speed PM motor. The major features of the motor are as described below.

(1) The magnetic bearings are applied for assuring the stabilized floating rotation control of the rotor at a high speed, reduction of bearing loss, and realizing lubricant-free and grease-less system.
(2) The Carbon Fiber Reinforced Plastics (CFRP) is applied as the material for the rotor sleeve to secure sufficient strength against centrifugal force and reduce the rotor eddy-current losses.

Table 1 Specifications of Prototype of High-Speed PM Motor

Specifications of the prototype of the high-speed PM motor are shown.

Item	Specifications
No. of poles	2
Rated output	250kW
Rated rotational speed	20,000min^{-1}
Frequency	333.3Hz
Rated torque	119.4N·m
Cooling system	Forced air cooling
Bearings	Magnetic levitation type

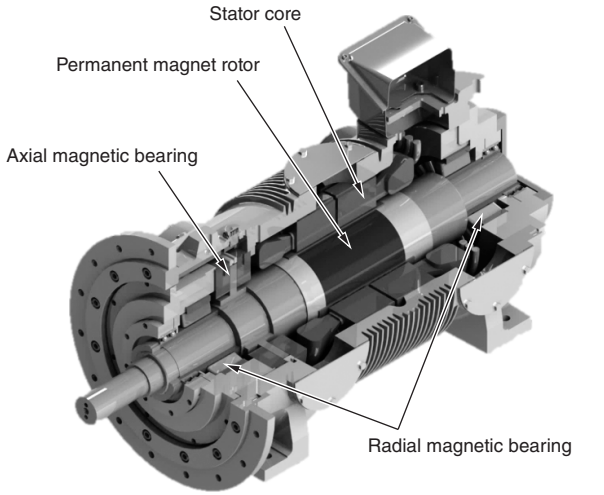

Fig. 1 Cross-Sectional Configuration of Prototype of High-Speed PM Motor

A cross-sectional configuration of the prototype of the high-speed motor is shown.

(3) By adopting a forced air cooling system using a cooling blower, it doesn't need to prepare a water or oil cooling circulation system.

3 Separation of No-Load Loss

We investigated approaches to separate the motor loss generated under the no-load conditions into each loss factor. For this time, we adopted two methods for loss separation. One was the method where the measured motor input power in no-load state was approximated by polynominal expression ("Separation by Polynominal Approximation"). The other was the method where the mechanical loss was directly measured with prepared the non-magnetized rotor ("Separation by Mechanical Loss Measurement").

3.1 Loss Separation by Polynominal Approximation

The input power for driving the motor in no-load state is equal to the no-load loss. Since the rotor shaft of the motor is levitated by the magnetic bearings, there will not be the friction loss due to contact between the rotor shaft and the bearings. The no-load loss, therefore, is separated roughly into windage loss, iron losses (eddy current loss and hysteresis loss), and copper loss.

The no-load loss, except included copper loss, is dependent on the rotational frequency. When the no-load loss is expressed in a cubic function of the rotational frequency, the tertiary term corresponds to windage loss[5], the secondary term corresponds to eddy current loss, and the primary term corresponds to hysteresis loss. Accordingly, characteristics of the no-load losses ($W_{NL\text{-}loss}$) for the rotational frequency (f) can be approximated into Expression (1) below. In this case, coefficients of the respective terms are assumed to be K_W, K_E, and K_H.

$$W_{NL\text{-}loss} = K_W \cdot f^3 + K_E \cdot f^2 + K_H \cdot f \cdots\cdots\cdots\cdots (1)$$

During the testing, no-load loss was measured at the intervals of 5000min^{-1}. Based on the actual measured values, coefficients of the respective terms can be derived from Expression (1), and then each loss at each rotational frequency was determined by the derive coefficients.

3.2 Loss Separation by Mechanical Loss Measurement

In this method, we firstly measured the mechanical loss by measuring the input power for rotating the non-magnetized rotor. Here, the mechanical loss includes the windage loss generated in the air gap and the iron loss generated in the magnetic bearings. And then the iron loss generated in the stator core of the motor in no-load state was determined by subtracting the value of measured mechanical loss from the one of total no-load loss at each rotational speed. In addition, the iron loss of the stator core can be separated into the eddy current loss and the hysteresis loss by polynominal approximation.

3.3 Result of No-Load Test

Fig. 2 shows the result of the separation of no-load loss assuming that total no-load loss at 20,000min^{-1} is 100%. Based on the separation by polynominal approximation, we confirmed that the rate of the windage loss and the eddy current loss

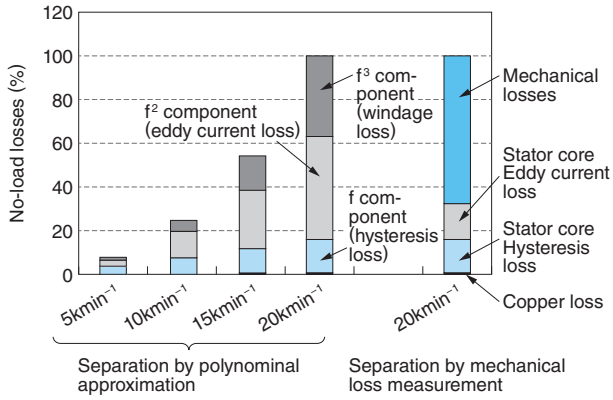

Fig. 2 Result of Separation of No-Load Loss

According to the result of loss separation by polynominal approximation, windage and eddy current losses account for more than 80% of total losses at 20,000min^{-1}. The result of loss separation by mechanical loss measurement indicates that about 68% of total losses are occupied by mechanical losses (windage loss and eddy current loss around magnetic bearings).

became larger as the rotational speed was increased and that the rate of those losses accounted for more than 80% of the total no-load loss at 20,000min^{-1}. Moreover, according to the separation by mechanical loss measurement, we confirmed that the mechanical loss accounted for about 68% of total no-load loss. Consequently, it is main factor to reduce the mechanical loss for improving the efficiency of the high-speed PM motor.

4 Back to Back Test

4.1 Method of Back to Back Test

Fig. 3 shows the state of coupling the two same specification prototypes for the back to back test. In order to calculate the shaft output and the motor efficiency, terminal voltages and currents of the two motors and also the both power of driving side (W_{in}) and regenerative side (W_{out}) were measured respectively by two power analyzers. The relation of W_{in} and W_{out} with the shaft output (W_{trg}) can be expressed by Expressions (2) and (3) below.

$$W_{in} = W_{trq} + (\textit{loss of the drive motor}) \cdots\cdots\cdots (2)$$

$$W_{out} = W_{trq} - (\textit{loss of the regeneration motor}) \cdots\cdots\cdots (3)$$

Since the terminal voltage and the current of the motor on driving side are almost the same with those on regenerative side at an output of W_{trq}, each motor loss generated on both side also can be assumed to be almost the same. On this assumption, Value W_{trg} can be derived from Expressions (2) and (3) and expressed into Expression (4) below.

$$W_{trq} = (W_{in} + W_{out})/2 \cdots\cdots\cdots (4)$$

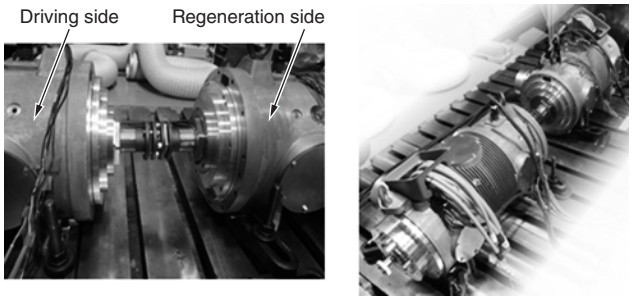

Fig. 3 State of Coupling for Back to Back Test

The state of coupling is shown, where two prototype models (the same type) are coupled.

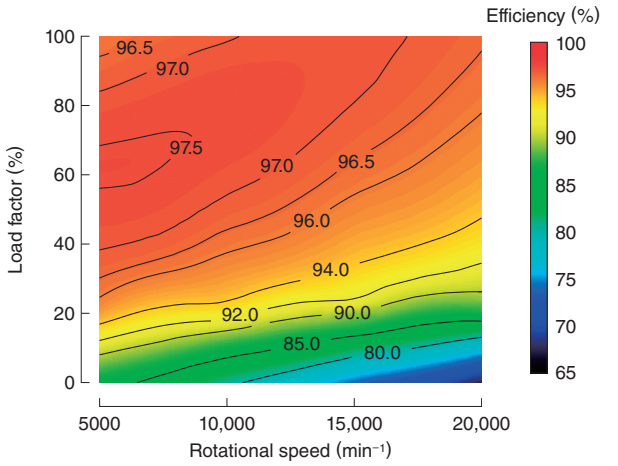

Fig. 4 Efficiency Map of Prototype Motor

The result of motor efficiency measurement performed during the load test is shown. This measurement was carried out for each set of rotational speed and load factor.

4.2 Load Characteristics

Based on the method as mentioned above, we measured the electrical characteristics and calculated the motor efficiencies while changing the rotational speeds and load factors up to the rated point of 250kW and 20,000min^{-1}. Fig. 4 shows the efficiency map of the prototype motor. Motor efficiency at the rated point was found to be 96.6% and the maximum efficiency in the whole motor operation range was 97.5%. As the result of the measurement, it is confirmed that the motor efficiency tends to be low in the high rotational speed region and it is considered that the cause of that is an influence of the losses that increase in proportion to the square or the cube of the rotational frequency as described in

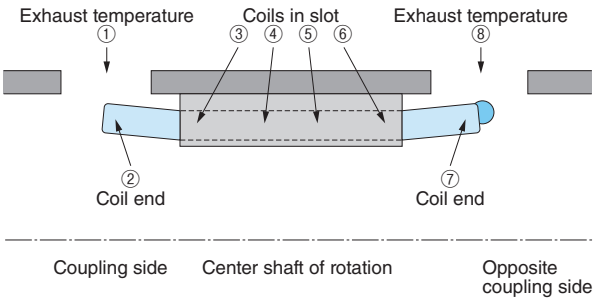

(a) Temperature measuring positions (Cross section in axial direction)

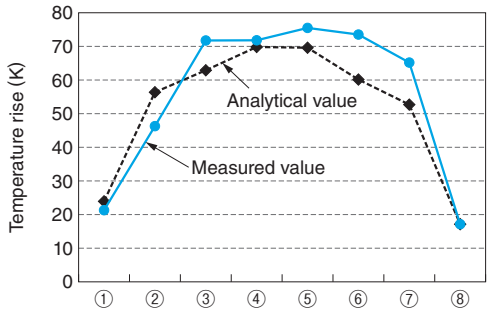

(b) Temperature rise values

Fig. 5 **Result of Temperature Rise Measurement in Each Part during Rated Operation**

The measurement result of temperature rise is shown. Temperature rise values were obtained from the respective parts of the motor body. (a) shows the specified temperature measuring points and (b) shows actual measured values and analytical values of temperature rise. These data suggest that sufficient cooling performance is secured.

Fig. 2. Therefore, we assume that it is the future task to investigate factors of increase in those losses and techniques for reducing the mechanical loss and the iron loss for improving the motor efficiency at especially high-speed region.

4.3 Heat Run Test

We carried out the heat run test at the rated point (250kW, 20,000min^{-1}) for measuring steady temperature rise of each part in the motor. Fig. 5 (a) shows cross section view in axial direction for indicating the points of measuring temperature and Fig. 5 (b) shows the both measured and analytical values of the temperature rise. In Fig. 5 (b), the analytical values were calculated by using a general Computational Fluid Dynamics (CFD) software and the measured values were obtained through thermocouples mounted at the respective measuring points.

As the result of the heat run test, we confirmed that temperature rises of each point in armature coil were lower than the specified level and the cooling performance was sufficient.

According to the comparison between analytical and measured values in Fig. 5, both gradients of temperature rise are almost equal, even though it seems that measured values tend to be slightly higher than the analytical values. As one possible cause, there was a difference of the loss distribution between the losses set in the analysis model and generated in actual state. In the high-speed rotation region, in particular, the proportion of windage loss and eddy current loss becomes high. It is, therefore, important to accurately estimate such losses in terms of estimating the temperature rise accurately.

5 Postscript

We have developed a prototype of 250kW-20,000min^{-1} high-speed PM motor. As the result of an evaluation, the motor efficiency at the rated point was found to be 96.6% and the maximum efficiency in the whole motor operation range was 97.5%. Further, we performed the loss separation and clarified the proportion of each loss in order to improve design accuracy.

In the future, we will work on further improving the accuracy of the loss separation for improving the motor efficiency and the accuracy of calculating the motor temperature with the thermal fluid analysis. Additionally, we will progress the development of higher speeds and larger capacities motors.

《References》

(1) Edition by the Advisory Committee for New Technologies toward Industrial Application of PM Motors: "New Technologies and Trends of Applications for the Extended Application Range with PM Motors," Journal of The Institute of Electrical Engineers of Japan, No.1207, 2010 (in Japanese)
(2) Edition by the Advisory Committee Related to Technologies of Ultra-High-Speed Drive and Bearing-Free Machinery: "The Latest Technologies of Ultra-High-Speed Drive and Bearing-Free Machinery," Journal of The Institute of Electrical Engineers of Japan, No.1058, 2006 (in Japanese)
(3) Uchiyama, Matsuo, Okitsu, Matsuhashi: "Characteristic Evaluation of a 250kW and 20,000min^{-1} High-Speed Motor," Meeting of The Institute of Electrical Engineers of Japan, No.5-020, 2016 (in Japanese)
(4) "The Ultimate Goal and Challenges of Speed-Controlled AC Drive Technologies," Journal of The Institute of Electrical Engineers of Japan, No.1326, 2014 (in Japanese)
(5) Takefumi Namai: Centrifugal Axial Flow Blowers and Compressors, Asakura Shoten, 1960 (in Japanese)